A double-gate heteromaterial tunnel FET optimized using an evolutionary algorithm

Sagarika Choudhury[1] · Brinda Bhowmick[1] · Krishna Lal Baishnab[1]

Abstract

A new technique is proposed herein for the design and optimization of double-gate heteromaterial tunnel field-effect transistors (FETs). The presented approach determines the optimum device dimensions, using a reference analytical model of the surface potential as an objective function. Many high-performance evolutionary optimization algorithms have been applied to determine optimum dimensions at reduced computational cost and complexity. A comparison of all these algorithms reveals particle swarm optimization to be the most suitable in terms of achieving an optimum surface potential at higher convergence speed. The optimized values are validated against technology computer-aided design (TCAD) simulation results, revealing acceptable values for the ON-current, and an OFF-current of 4.8×10^{-15} A in accordance with International Technology Roadmap for Semiconductor (ITRS) 2014 requirements. The subthreshold slope is found to be 45 mV/dec. The algorithm dynamically fixes the lengths of the source, channel, and drain junctions, device thickness, etc. The automated determination of these parameters can effectively improve the computational complexity while providing accurate designs for tunnel field-effect transistors.

Keywords Band-to-band tunneling · Evolutionary algorithms · PSO · Optimization

1 Introduction

The downscaling of metal–oxide–semiconductor field-effect transistors (MOSFETs) has resulted in some serious issues, such as drain-induced barrier lowering (DIBL), high OFF-current and subthreshold swing (SS), as well as several other distinct short-channel effects (SCEs). Hence, tunnel field-effect transistors (TFETs) are being considered as an alternate to overcome such drawbacks of MOSFETs [1–5]. TFETs are well known for their steeper SS [6] and low OFF-current (I_{OFF}) [7], but suffer from a lower ON-current than required by the ITRS [8]. Many novel structures have been reported to improve the ON-current of TFETs. However, when applying traditional approaches [6, 7], such structures are optimized using trial-and-error methods. The derivation of analytical expressions for a particular electrical parameter followed by the use of optimization techniques on them to

obtain the best device dimensions would thus represent a great achievement. The derivation of an optimal solution when designing a TFET involves many approximations, making the process tiresome and lengthy. The application of optimization algorithms [9–11] to identify an optimized structure is thus a convenient option to improve the computational efficiency of the design process. Their good approximation ability and high convergence speed have resulted in the use of various evolutionary and behavior-based optimization techniques to solve problems in real time [9–11].

No work has been carried out to optimize the dimensions of TFET designs using algorithms, with trial-and-error techniques always being applied to determine optimum device dimensions. In the work presented herein, a TFET model based on an analytical surface potential presented in Ref. [12] is applied. The surface potential is chosen because it plays an important role in determining the electric field in the tunnel junction, which greatly affects the tunneling probability. A number of efficient algorithms, viz. particle swarm optimization (PSO) [13], differential evolution (DE) [14], human behavior-based PSO (HBPSO) [15], and hybrid DEPSO [16], are thus used to find the optimum surface potential, thereby obtaining the optimum dimensions

✉ Sagarika Choudhury
  sagarikachoudhury36@gmail.com

1   Department of Electronics and Communication Engineering,
    National Institute of Technology, Silchar, Silchar,
    Assam 788010, India

for the proposed TFET. Next, to validate the accuracy of the proposed method, a device with the obtained dimensions is designed in TCAD software. A comparison with the reference confirms the effectiveness of the proposed method. The remainder of this manuscript is organized as follows: In Sect. 2, the objective function, design variables, and optimization algorithms are described. The results, analysis, and validation are elaborated in Sect. 3. The optimized device structure is reported in Sect. 4. Finally, the conclusions that can be drawn from this work are highlighted in Sect. 5.

2 Analytical model

The analytical model for the surface potential obtained from Ref. [12] is used as the objective function, expressed as

$$\psi_s(x) = B \exp(px) + C \exp(-px) + \psi_k, \tag{1}$$

where ψ_k is the one-dimensional (1D) surface potential, and B and C are constants given by the following equations:

$$B = \frac{1}{K} \left\{ \begin{array}{c} 2\left(-\psi_k - \frac{qN_D L_1^2}{2\varepsilon}\right) \sinh p(L_2 - L_3) - 2(\varphi_1 - \psi_k) \\ -L_1 p(\varphi_1 - \psi_k)e^{-p(L_1 - L_2)} + q\frac{N_D L_1^2}{\varepsilon}e^{p(L_2 - L_3)} \\ +2(\varphi_2 + V_{DS} - \psi_k)\sinh p(L_3 - L_1) \end{array} \right\}, \tag{2}$$

$$C = \frac{(\varphi_2 + V_{DS} - \psi_k)e^{pL_3} - e^{pL_2}(\varphi_1 - \psi_k)}{K}, \tag{3}$$

$$K = 2\sinh p(L_2 - L_3), \tag{4}$$

$$p^2 = \frac{\varepsilon^*}{\varepsilon \tau t_s}, \tag{5}$$

where φ_1 and φ_2 are potentials that are determined by considering the external potential applied at $x = 0$ and $x = L_3$.

As seen from this equation, the optimum value of x for which $\psi_s(x)$ is optimized must be found, thus the optimum values for L_1, L_2, and L_3, which are part of x, must be found.

2.1 The effect of varying L_1, L_2, and L_3

To understand the effect of the variation of the lengths, L_1, L_2, and L_3 are not used as the design variables; rather, they are found analytically by a trial-and-error method. The only design variable is x. Equation 1 is optimized for different combinations of lengths using two optimization techniques. The results are presented in Table 1, revealing that the combination $L_1 = 0.01x$, $L_2 = 0.91x$, $L_3 = 0.08x$ is more optimal, because increasing the value of L_1 or L_3 and decreasing L_2 increases the surface potential. Further combinations of the three lengths were tried, but the results were very large. Thus, based on this analysis, it is observed that L_1, L_2, and L_3 play a major role in changing the surface potential, indicating the importance of optimizing their values.

2.2 The determination of the surface potential using computationally efficient algorithms

The surface potential plays an important role in TFET design. In this work, the analytical expression for the surface potential is taken from Ref. [12]. However, it is observed that obtaining the optimum dimensions for the proposed device is a tedious process. So, it is necessary to enhance the computational efficiency of this process. In this work, various computationally efficient evolutionary algorithms are applied to optimize the expression for the surface potential and thus obtain the optimal device dimensions. These metaheuristics-based algorithms achieve better accuracy in comparison with other mathematical techniques for the solution of technical problems in real time. Therefore, the discussed algorithms are found to be most suitable in terms of their approximation to the optimum, computational complexity, and convergence speed [9–11, 13–17]. The algorithms considered herein include the particle swarm optimization (PSO) algorithm

Table 1 The effect of varying the lengths on the surface potential

Arbitrary values of L_1, L_2, and L_3	Variable	Range (nm)	PSO-based optimum x (nm)	PSO-based optimum surface potential (V)	DE-based optimum x (nm)	DE-based optimum surface potential (V)
$L_1 = 0.01x$ $L_2 = 0.91x$ $L_3 = 0.08x$	x	0–35	35	0.73	30.24	0.670
$L_1 = 0.01x$ $L_2 = 0.9x$ $L_3 = 0.09x$	x	0–35	35	1.0226	27.59	1.09
$L_1 = 0.02x$ $L_2 = 0.9x$ $L_3 = 0.08x$	x	0–35	35	4.89	17.19	1.2533

described by Kennedy and Eberhart [13], the differential evolution (DE) algorithm described by Storn and Price [14], a human behavior-based PSO algorithm (HBPSO) described by Liu et al. [15], a hybrid DE and PSO algorithm (DEPSO) described by Jhang and Xi [16], and Salp Swarm Algorithm (SSA) [17]. A comparative analysis among the results obtained using these algorithms indicates that PSO is the most efficient for obtaining the desired value of the surface potential in terms of the percentage error and convergence speed. Figure 1 depicts the flowchart of the PSO algorithm.

2.3 The estimation of the design variables and their ranges

The expression for the surface potential in Eq. (1) is used as an objective function along with the design constraints explained in Eqs. (2–5) as well as in Eq. (6):

$$x = L_1 + L_2 + L_3. \tag{6}$$

Using this equation, the design variables can be obtained as

$$X_{\text{TFET}} = \begin{bmatrix} L_1, L_2, L_3, x, t_s, V_{\text{DS}} \end{bmatrix}$$

The design variables are chosen judiciously to reduce the computational time. The parameters which play a vital role in the performance of the TFET with respect to the surface potential are chosen as the design variables. Thus, six design variables are obtained, as listed in Table 2. As explained in Sect. 2.1, the lengths L_1, L_2, and L_3 at various points in x affect the value of the surface potential and are thus major factors affecting it. Therefore, to optimize the surface potential, these lengths must also be optimized. The ranges of the design variables are formulated based on the ITRS, whereas other design limitations are not incorporated. Thereby, the optimized values should lie within the ranges presented in Table 2. The constants in the objective function are presented in Table 3.

2.4 The parameters used in the optimization algorithms

The values of the parameters used in the algorithms to solve the objective function are described as follows:

(a) For PSO and DEPSO, the social learning rate (c_1) is taken as 0.12, while the cognitive learning rate (c_2) is 1.2, keeping a dimension of 6 and swarm size of 100.

(b) For DE, the mutation factor (F) is taken as 0.5 with a crossover rate of 0.9 for a population size of 100 with dimension of 6.
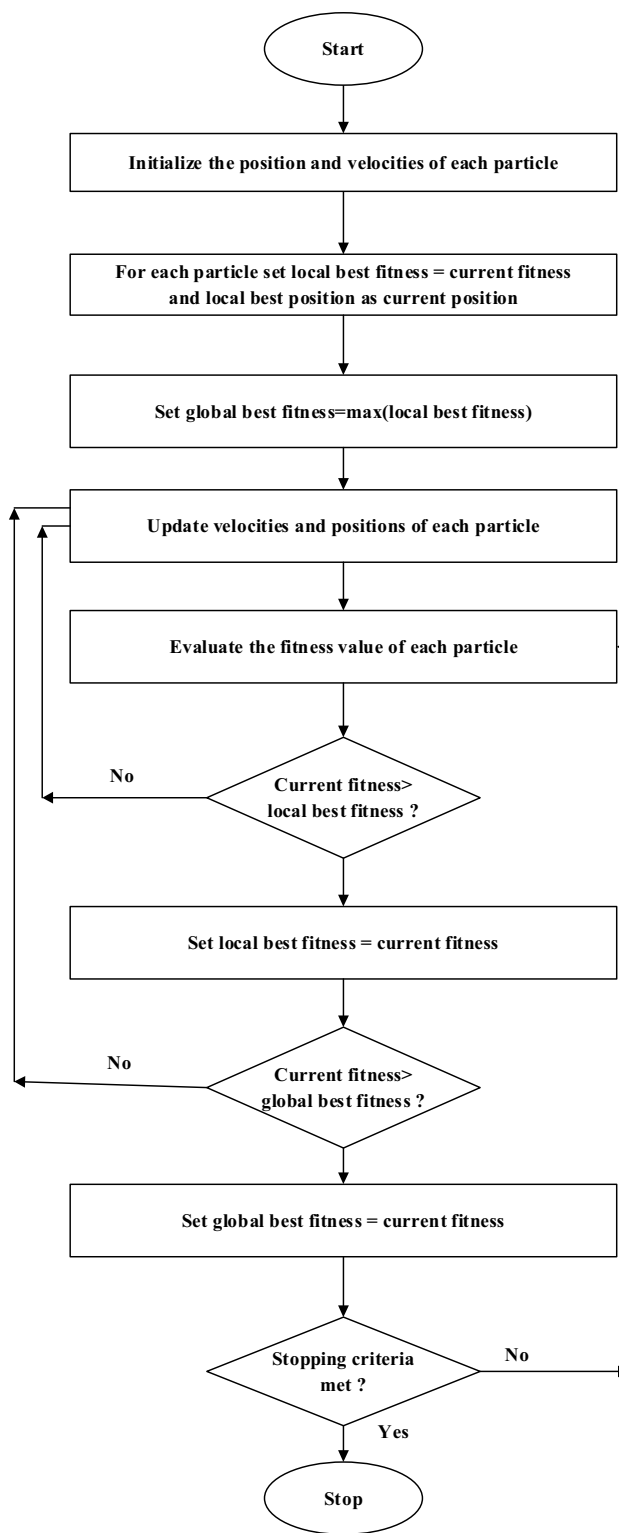

Fig. 1 The flowchart of the PSO algorithm

Table 2 The design variables and their ranges

Variable	Range
L_1 (nm)	$(0.01–0.99) \times x$
L_2 (nm)	$(0.01–0.99) \times x$
L_3 (nm)	$(0.01–0.99) \times x$
x (nm)	0–35
t_s (nm)	10–40
V_{DS} (V)	0.5–1.2

Table 3 The design constants of the proposed TFET structure

Parameter	Symbol	Dimension
Device layer thickness	t_s	20×10^9 nm
Absolute permittivity	ε_0	8.854×10^{12}
Relative permittivity of SiO_2	ε^*	$3.9 \times \varepsilon_0$
Relative permittivity of medium	ε	$11.4 \times \varepsilon_0$
Donor concentration in drain region	N_d	5×10^{18} cm^{-3}
Electronic charge	q	1.6×10^{-19}
phi_1	φ_1	0
phi_2	φ_2	1.2

(c) For SSA, 50 search agents are used with dimension of 6.

(d) HBPSO is implemented with a population size of 100 and a dimension of 6.

3 The optimization results and their analysis

The objective function defined in Sect. 2 is solved to determine the optimized values for the design variables specified in Table 2. The simulations are performed in MATLAB 2013 on a processor with speed of 3.4 GHz. The resulting optimum values are presented in Table 4, revealing that the PSO algorithm offers the best performance with a minimum error, as shown in Fig. 4. The algorithms are compared based on convergence plots in Fig. 2. The optimum results obtained by the PSO algorithm are validated by designing a double-gate heteromaterial tunnel FET in Synopsys TCAD using the optimum dimensions and the remaining parameters
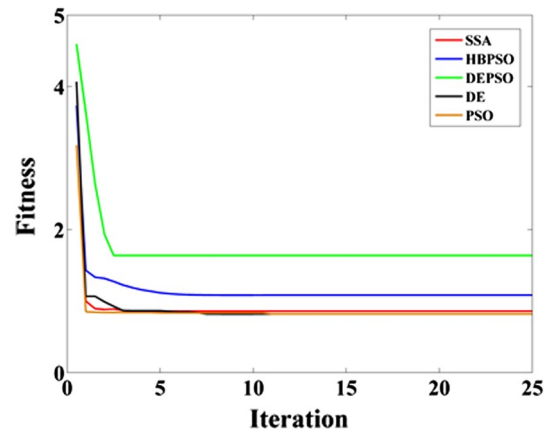

Fig. 2 The convergence plots of the different algorithms

from our work. The range for the surface potential in the TCAD simulation is 0.5–0.9 V, as mentioned in Ref. [12], being almost equal to that obtained using the PSO algorithm as shown in Fig. 3. The simulation results obtained in MATLAB and TCAD differ by a smaller range during the construction of the tunnel FET because some parameters are rounded off to the nearest decimal values (Figs. 4, 5). The simulation plots and results in Figs. 6, 7 and 8 are obtained from TCAD simulations, validating the obtained result as optimum when compared with the design specification.

3.1 Validation using TCAD software

As explained in Sect. 3, the PSO algorithm provides the best value of the surface potential. So, the device structure is simulated in TCAD using the values of the design variables obtained using this algorithm. Figure 6 shows the linear I_D–V_{GS} characteristic of the device with the optimized dimensions. Figure 7 shows the log I_D versus V_{GS} characteristic of the optimized device, revealing an ON-current of 4.8×10^{-4} A and an OFF-current of 4.8×10^{-15} A. Figure 8 shows the surface potential of the optimized device. The subthreshold slope is found to be 45 mV/dec.

Table 4 The optimized values of the design variables

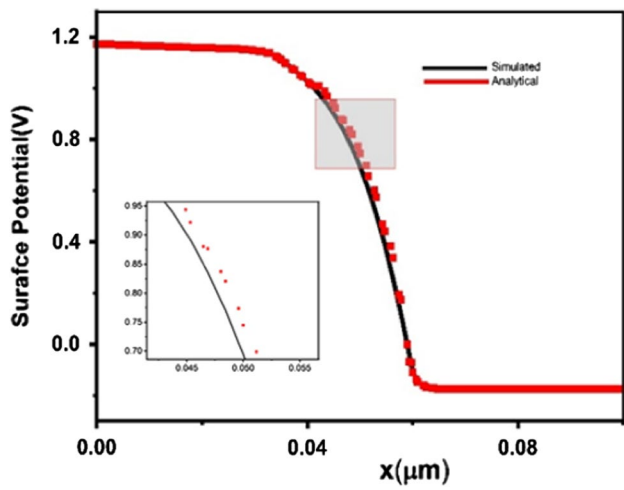| Design variables	Range	PSO	DE	HBPSO	DEPSO	SSA
L_1 (nm)	$(0.01–0.99) \times x$	0.700×34	0.0100×33.56	0.0100×34.25	0.0100×34.25	0.0100×34
L_2 (nm)	$(0.01–0.99) \times x$	0.20×34	0.955×33.56	0.9800×34.25	0.9800×34.25	0.9800×34
L_3 (nm)	$(0.01–0.99) \times x$	0.10×34	0.035×33.56	0.0100×34.25	0.0100×34.25	0.0200×34
x (nm)	0–35	34	33.56	34.25	34.25	34
t_s (nm)	10–40	25	38.66	40	40	39.72
V_{DS} (V)	0.5–1.2	0.7	0.55	0.52	0.52	0.51

Fig. 3 A plot of the simulated versus reference surface potential
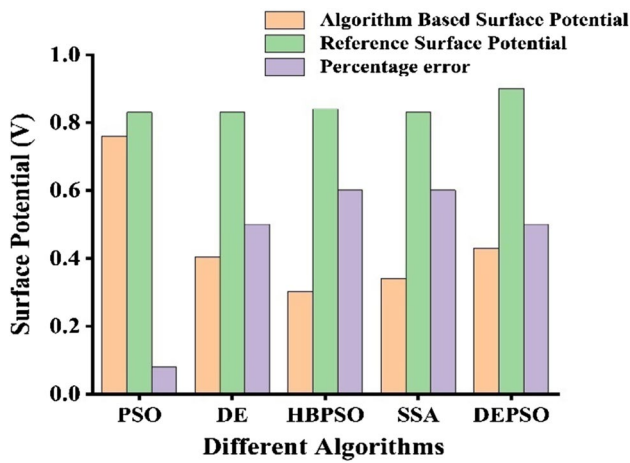

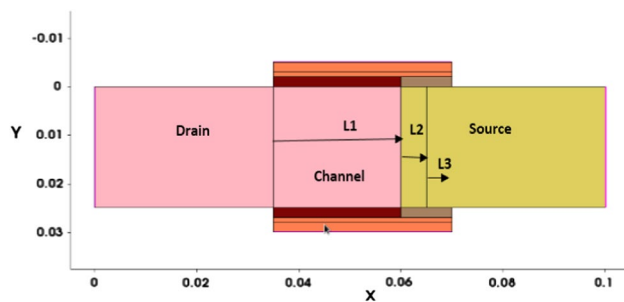**Fig. 4** The percentage error in the surface potential computation at $x = 34$ nm
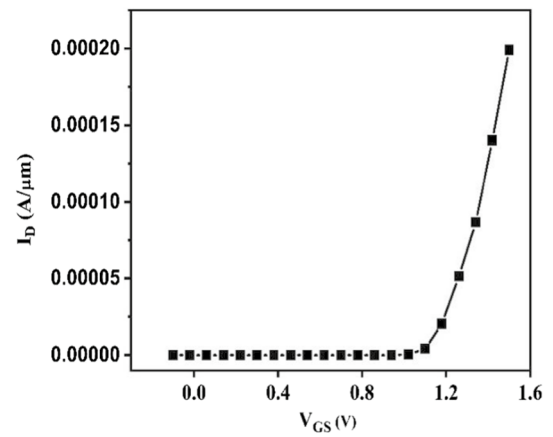

Fig. 5 The proposed optimized structure

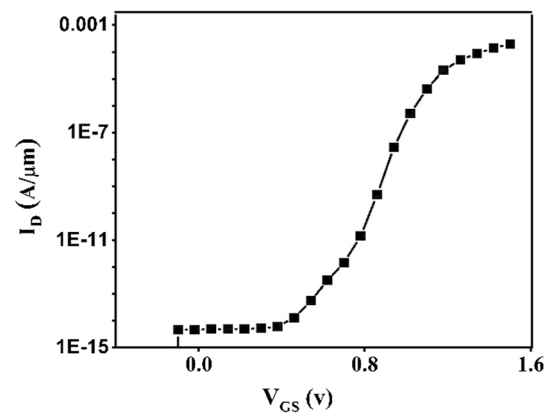**Fig. 6** The linear I_D–V_{GS} curve of the proposed device

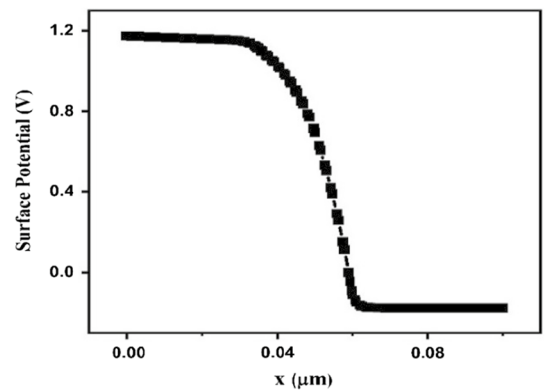**Fig. 7** The log I_D–V_{GS} curve of the proposed device

Fig. 8 The surface potential of the proposed design

4 The proposed architecture of the device

The proposed structure incorporates a *p*-type germanium source, *n*-type drain, and intrinsic channel, as shown in Fig. 5. The structure is designed with a heterogate dielectric, having a low-*k* gate oxide (SiO_2) on the drain side to reduce the ambipolar current and a high-*k* oxide (HfO_2) at the tunneling junction. An N^+ polysilicon electrode with work function of 4.5 eV is used as the gate electrode. To increase the tunneling probability, the source side is designed with a low-bandgap material (germanium). The device is operated with its source grounded, 1.5 V applied to the gates, and the drain connected to 0.7 V. The dimensions of the device are obtained using the optimization techniques as explained in the previous section. The doping concentration of the source, channel, and drain is 10^{20}, 10^{16}, and 5×10^{18} cm^{-3}, respectively. The length L_1 represents the channel region under the SiO_2 gate oxide, which is a lightly doped region; L_2 is the source depletion region, and L_3 is the source region beneath the HfO_2 gate oxide.

5 Conclusions

A mathematical model for the surface potential is obtained from Ref. [12], and the optimum device dimensions are determined using optimization algorithms. Various optimization techniques are applied to determine the optimum device dimensions for a double-gate tunnel FET. TCAD simulations are carried out on the device with the optimized dimensions. The values of the surface potential obtained from the simulated design for various values of *x* match those given in the reference paper. The ON-current, OFF-current, and subthreshold swing values are also obtained from the simulation. A comparison with Ref. [12] confirms the good accuracy of the proposed model, with the PSO method offering improved accuracy. A small deviation arises due to the inability to implement precise values of the obtained dimensions in the simulation tool. The effectiveness and accuracy of the computation are improved by using the proposed methodology.

References

1. Seabaugh, C., Zhang, Q.: Low-voltage tunnel transistors for beyond CMOS logic. Proc. IEEE **98**, 2095–2110 (2010)
2. Koswatta, S.O., Lundstrom, M.S., Nikonov, D.E.: Performance comparison between p-i-n tunneling transistors and conventional MOSFETs. IEEE Trans. Electron Devices **56**, 456–465 (2009)
3. Toh, E.H., Wang, G.H., Samudra, G., Yeo, Y.C.: Device physics and design of germanium tunneling field-effect transistor with source and drain engineering for low power and high performance applications. J. Appl. Phys. **103**, 104504-1–104504-5 (2008)
4. Kumar, M.J., Janardhanan, S.: Doping-less tunnel field effect transistor: design and investigation. IEEE Trans. Electron Devices **60**, 3285–3290 (2013)
5. Saurabh, S., Kumar, M.J.: Estimation and compensation of process-induced variations in nano scale tunnel field-effect transistors for improved reliability. IEEE Trans. Device Mater Reliab. **10**, 390–395 (2010)
6. Choi, W.Y., Park, B.G., Lee, J.D., Liu, T.J.K.: Tunneling field effect transistors (TFETs) with sub threshold swing (SS) less than 60 mV/dec. IEEE Electron Device Lett. **28**, 743–745 (2007)
7. Lonescu, A.M., Riel, H.: Tunnel field-effect transistors as energy efficient electronic switches. Nature **479**, 329–337 (2011)
8. International Technology Roadmap for Semiconductor (2014)
9. Yu, X., Gen, M.: Introduction to Evolutionary Algorithms. Springer, London (2010)
10. Nelder, A.J., Mead, R.: A simple method for function optimization. Comput J **7**, 238–252 (1965). https://doi.org/10.1093/comjnl/7.4.308
11. Rao, S.S.: Engineering Optimization Theory and Practice. Wiley, New York (2009)
12. Bhowmick, B., Baishya, S.: A physics-based model for electrical parameters of double gate hetero-material nano scale tunnel FET. Int. J. Appl. Inf. Syst. (IJAIS) **1**(3). https://doi.org/10.5120/ijais12-450142
13. Kennedy, J., Eberhart, R.C.: Particle swarm optimization. In: Proc IEEE International Conference on Neural Networks, pp. 1942–1948 (1995)
14. Storn, R., Price, K.: Differential evolution—a sample and efficient adaptive scheme for global optimization over continuous spaces. In: International Computer Science Institute. Technical report, 95- 012, Berkley, March, pp. 1–11 (1995)
15. Hao, L., Gang, X., Ding, Y.G., Sun, Y.B.: Human behavior based particle swarm optimization. Sci. World J. (2014). https://doi.org/10.1155/2014/194706
16. Zhang, W.J., Xie, X.F., DEPSO: Hybrid particle swarm with differential evolution operators. In: Proceedings of the IEEE International Conference on System, Security and Assurance, pp. 3816–3821 (2003)
17. Mirjalili, S., Gandomi, A.H.: Salp Swarm Algorithm: a bio-inspired optimizer for engineering design. Adv. Eng. Softw. **114**, 163–191 (2017)